Figure S7

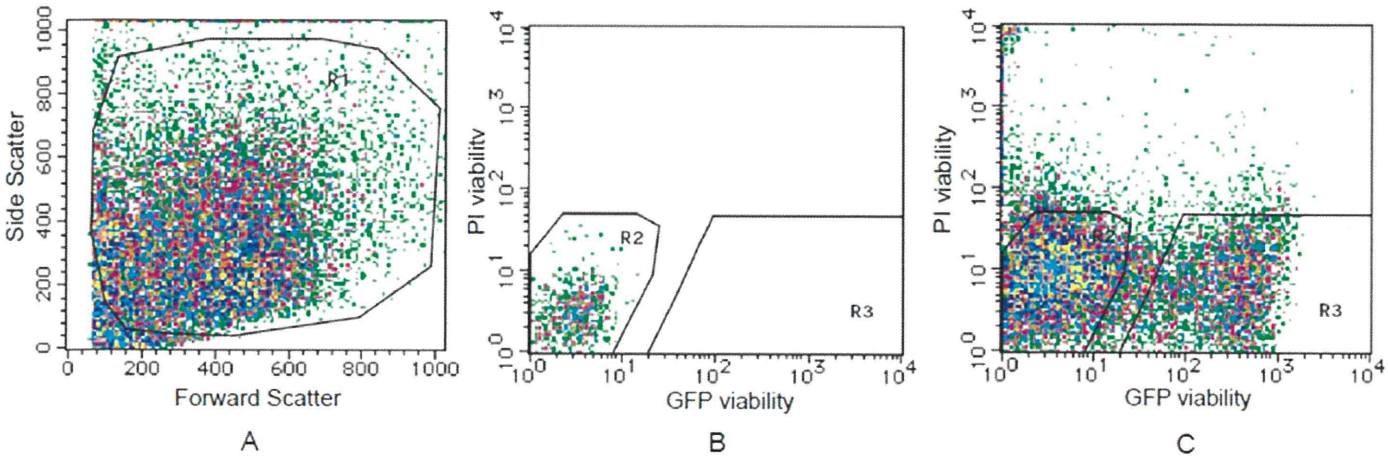

A B C

Table S1 Sequence of specific primers for RT-PCR.

Gene		Sequence
EGFP	forward	5'-CGACAAGCAGCAGAAGAACGGCATCAA-3'
	reverse	5'-ACGAACTCCAGCAGGACCATGTGA-3'
Gapdh	forward	5'-GGAGCCAGACCCCACTAACA-3'
	reverse	5'-GCCTTCTCCATGGTGGTGAA-3'
Otx1	forward	5'-GCTTCTTCGTCTAGCTCAGC-3'
	reverse	5'-AGGCTTGGTCCTTATAGTCC-3'
Otx2	forward	5'-CCTCTAGTACCTCAGTCCCAA-3'
	reverse	5'-GTCCATTTCAGGTTGCTGGT-3'
Prr15	forward	5'-TTGAAGATCTCACGCTCTGG-3'
	reverse	5'-GGTGACACCTCCGAATGACT-3'
Gbx2	forward	5'-AGACGGCAAAGCCTTCTTG-3'
	reverse	5'-GGGTCATCTTCCACCTTTGA-3'
Prrx2	forward	5'-GTGTATTTGAGCGCACACAC-3'
	reverse	5'-GGCCTTAGGCACAATCTCAG-3'
Isl1	forward	5'-ATGGTGGTTTACAGGCTAACC-3'
	reverse	5'-CATCTGAATGAATGTTCCTCATGCC-3'
Bmp4	forward	5'-TAGGTGAGTTCGGCATCCGA-3'
	reverse	5'-TGTTCTCCAGATGTTCTTCG-3'
Jag1	forward	5'-CAGAATGACGCCTCCTGTCG-3'
	reverse	5'-TGCAGCTGTCAATCACTTCG-3'
Lfng	forward	5'-CCATTCTCTGTGGAAGCTGA-3'
	reverse	5'-CAGGGACAGAGTTTCAACCA-3'
Neurog1	forward	5'-CCGACGACACCAAGCTCA-3'
	reverse	5'-CTTCAGCCAGTTCCCCATCT-3'
Sox2	forward	5'-GAAAGAAAGGAGAGAAGTTTGGAG-3'
	reverse	5'-GAAGTGCAATTGGGATGAAA-3'
Espn	forward	5'-CTGCCTGGAGACGAGACATT-3'
	reverse	5'-GACTGTTCTTTCGCCCTCTG-3'
Myo7a	forward	5'-GTGGTCAATTATGCCCGTTT-3'
	reverse	5'-GCTCGTCCACGAAGTACACA-3'
Eya4	forward	5'-TCACAACAAATGGGACAGGA-3'
	reverse	5'-AAGTGTCAAGCGCTCCATCT-3'
Eya1	forward	5'-CGGAAGCAGCAGCTTTAGTC-3'
	reverse	5'-GTGAGGAAGGGGAGGGAGA-3'
Gata3	forward	5'-AGGGAGTGTGTGAACTGGGG-3'
	reverse	5'-GGTCGGAGGAACTCTTCGCA-3'
Lect1	forward	5'-ACAGTGGGATAGGGTCTTCG-3'
	reverse	5'-TCCCAGTGATGCCATTTTTA-3'
Tnfrsf12a	forward	5'-CAGATCCTCGTGTTGGGATT-3'
	reverse	5'-AATGAATGAATGGACGACGAG-3'

Table S2 P value of one-way ANOVA among homozygous, heterozygous Line 14 mice and wild type controls for ABR threshold in 2, 4, 8, 16, 32kHz.

	P value
2kHz	0.967
4kHz	0.934
8kHz	0.956
16kHz	0.857
32kHz	0.655

Jaw muscularization requires *Dlx* expression by cranial neural crest cells

Églantine Heude[a], Kamal Bouhali[a], Yukiko Kurihara[b], Hiroki Kurihara[b], Gérard Couly[a], Philippe Janvier[c,d], and Giovanni Levi[a,1]

[a]Évolution des Régulations Endocriniennes, Centre National de la Recherche Scientifique Unité Mixte de Recherche 7221, Muséum National d'Histoire Naturelle, 75005 Paris, France; [b]Department of Physiological Chemistry and Metabolism, Graduate School of Medicine, University of Tokyo,113-0033 Tokyo, Japan; [c]Département Histoire de la Terre, Centre National de la Recherche Scientifique Unité Mixte de Recherche 7207, Muséum National d'Histoire Naturelle, 75005 Paris, France; and [d]The Natural History Museum, London SW7 5BD, United Kingdom

Edited* by Nicole M. Le Douarin, Centre National de la Recherche Scientifique, Gif-sur-Yvette, France, and approved May 14, 2010 (received for review February 11, 2010)

The origin of active predation in vertebrates is associated with the rise of three major, uniquely derived developmental characteristics of the head: (*i*) migratory cranial neural crest cells (CNCCs) giving rise to most skeletal skull elements; (*ii*) expression of *Dlx* genes by CNCCs in the *Hox*-free first pharyngeal arch (PA1); and (*iii*) muscularization of PA1 derivatives. Here we show that these three innovations are tightly linked. Expression of *Dlx* genes by CNCCs is not only necessary for head skeletogenesis, but also for the determination, differentiation, and patterning of cephalic myogenic mesoderm leading to masticatory muscle formation. In particular, inactivation of *Dlx5* and *Dlx6* in the mouse results in loss of jaw muscles. As *Dlx5/6* are not expressed by the myogenic mesoderm, our findings imply an instructive role for *Dlx5/6*-positive CNCCs in muscle formation. The defect in muscularization does not result from the loss of mandibular identity observed in *Dlx5/6*$^{-/-}$ mice because masticatory muscles are still present in *EdnRA*$^{-/-}$ mutants, which display a similar jaw transformation. The genesis of jaws and their muscularization should therefore be seen as an integrated *Dlx*-dependent developmental process at the origin of the vertebrate head. The role of *Dlx* genes in defining gnathostome jaw identity could, therefore, be secondary to a more primitive function in the genesis of the oral skeletomuscular system.

craniofacial development | Dlx5-Dlx6 | myogenesis | mesoderm | evolution

During chordate evolution, innovations specific to vertebrates permit the apparition of the "new head" (1), a neomorphic unit endowed with a muscularized oral structure that allows the transition from filter feeding to active predation. The considerable selective advantage of predatory capacity in vertebrates goes together with the presence of *Hox*-negative skeletogenic cranial neural crest cells (CNCCs) migrating in the cephalic region (2, 3). The CNCC-derived cephalic skeletal elements need to associate with contractile muscles to give rise to a functional mouth. The question of how oral skeletal and muscular morphogenesis is coordinated is, therefore, central for understanding the origin of active predation during vertebrate evolution.

Craniofacial shapes are amazingly diverse among different vertebrate groups and also within individual species (4, 5). In all cases, however, vertebrates are characterized by a muscularized functional mouth, suggesting a tight link between skeletal elements derived from the CNCCs and craniofacial muscles of mesodermal origin. The possible interaction between CNCCs and the mesoderm in orchestrating craniofacial myogenesis was suggested several years ago (6). Only recently, however, has it been demonstrated that CCNCs can regulate muscle progenitors in the head and participate in shaping the cranial musculoskeletal architecture in vertebrate embryos (7–9).

Head muscles have various embryonic origins: in tetrapods, the tongue derives from the rostral migration of anterior somitic mesoderm; other skeletal muscles derive from cranial paraxial mesoderm (CPM) (10, 11) and from lateral splanchnic mesoderm (SpM) (12). Remarkably, the development of cephalic and trunk muscles depends on different regulatory pathways (13–16). In the head, bone morphogenetic proteins (BMPs) and canonical Wnt signaling molecules act to repress skeletal muscle differentiation. By contrast, the same BMP and Wnt ligands are required to stimulate myogenesis in the trunk. Myogenic differentiation of the CPM in vitro is permitted, therefore, by CNCC production of BMP and Wnt inhibitors (Noggin, Gremlin, Frzb) (17). Both the head skeleton and the head musculature are therefore different from their truncal counterpart, reinforcing the notion that the "new head" has been a recent addition to a primitive body plan (1).

CNCCs and mesodermal cells colonizing the first pharyngeal arch (PA1) and more anterior structures do not express *Hox* genes (18); their patterning depends on the expression of non-*Hox* homeobox genes including *Distal-less* (*Dlx*) transcription factors (19). In particular, *Dlx5* and *Dlx6* are necessary and sufficient to specify PA1 skeletal maxillo-mandibular identity in gnathostomes: in their absence mandibular skeletal structures are transformed into maxillary elements (20, 21), and their activation in the maxillary arch leads to embryos with four opposing mandibles (22). *Dlx5/6* expression is restricted to CNCCs (23) and is not observed in the myogenic mesoderm (Fig. S1). Early *Dlx5/6* activation in PA1 depends on endothelin 1 (Edn1) signaling from the endoderm: mice lacking *Edn1* or its receptor A (*EdnRA*) present a skeletal transformation reminiscent of that observed in *Dlx5/6* double mutants (24, 25).

Given the key role of *Dlx5* and *Dlx6* in determining PA1 identity, we used *Dlx5/6* and *EdnRA* mutant mice to analyze how CNCCs control head muscle morphogenesis. We show that craniofacial myogenesis depends on *Dlx5/6* expression by CNCCs, but is not directly related to the PA1 maxillo-mandibular identity. The results suggest that *Dlx* genes might have had a central role in coordinating the development of the oral skeleto-muscular apparatus at the origin of active predation in vertebrates.

Results

Inactivation of Either *Dlx5/6* or *EdnRA* in the Mouse Results in Head Muscle Malformations. Histo-anatomical analysis of embryonic day 18.5 (E18.5) *EdnRA*$^{-/-}$ and *Dlx5/6*$^{-/-}$ mutant heads shows that the skeletal malformations are associated with severe muscle defects (Fig. 1, Fig S2, and Table S1). In *Dlx5/6*$^{-/-}$ double-mutant mice, all PA1-derived masticatory muscles and PA2-derived muscles are absent and replaced by undifferentiated reticular connective tissue (Fig. 1 *C* and *C′* and Fig. S2*G*). This

Author contributions: É.H., G.C., and G.L. designed research; É.H. and K.B. performed research; H.K. and Y.K. contributed new reagents/analytic tools; É.H., K.B., H.K., Y.K., G.C., P.J., and G.L. analyzed data; and É.H., P.J., and G.L. wrote the paper.

The authors declare no conflict of interest.

*This Direct Submission article had a prearranged editor.

[1]To whom correspondence should be addressed. E-mail: glevi@mnhn.fr.

This article contains supporting information online at www.pnas.org/lookup/suppl/doi:10.1073/pnas.1001582107/-/DCSupplemental.

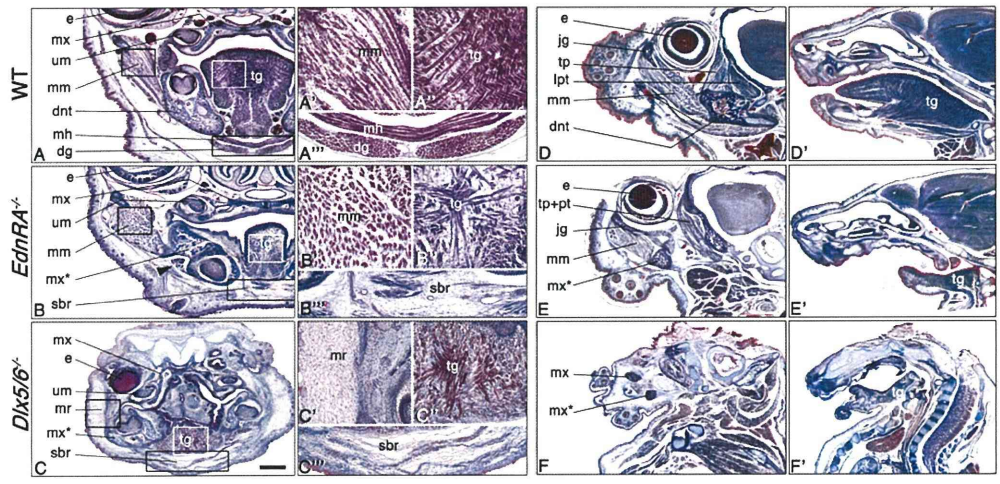

Fig. 1. Head muscle phenotypes observed in *EdnRA*$^{-/-}$ and *Dlx5/6*$^{-/-}$ mutant mice. Mallory trichromic staining on frontal (*A–C*) and parasaggital (*D–F*) sections of E18.5 wild-type, *EdnRA*$^{-/-}$, and *Dlx5/6*$^{-/-}$ mice. The *EdnRA*$^{-/-}$ and *Dlx5/6*$^{-/-}$ mutants show a duplicated maxillary bone (mx*) associated with head muscle defects. In the *EdnRA*$^{-/-}$ mutant, the masseter muscle (mm) is present but has an abnormal morphology and orientation (*B–B′* and *E*); all masseter components pass through the infraorbital foramen of the transformed lower jaw (black arrowhead in *B*). The pterygoid and temporal muscles are indistinguishable and form a single muscular mass (*E*). In the *Dlx5/6*$^{-/-}$ mutant, the masseter muscle is replaced by connective tissue [see the masseter region (mr) in *C* and *C′*]. In the two mutants, the tongue is considerably reduced, the muscles fibers are totally disorganized (*B*, *B″*, *C*, *C″*, *E′*, and *F′*), and sublingual muscles are either absent or replaced by a few muscle fibers (*B‴* and *C‴*). dg, digastric muscle; dnt, dentary bone; e, eye; jg, jugal bone; lpt, lateral pterygoid muscle; mh, mylohoid muscle; mm, masseter muscle; mr, masseter region; mx, maxillary bone; mx*, duplicated maxillary bone; pt, pterygoid muscle; sbr, sublingual region; tg, tongue; tp, temporal muscle; um, upper molar. (Scale bar: 500 μm in *A–C*; 700 μm in *D–F* and *D′–F′*; 100 μm for other panels.)

observation contrasts sharply with the persistence of transformed jaw skeletal elements that are therefore devoid of any muscular connection. Oculo-motor muscles are present, but their morphology is altered in parallel with eye malformations (Fig. 1*C*). More posterior muscles are also present, but their morphology is altered and individual muscle masses are not identifiable (Fig. 1 *D* and *F*).

In *EdnRA*$^{-/-}$ mutants, masticatory muscles are present, but their morphology is perturbed (Fig. 1 *B*, *B′*, and *E*; Fig. S2*D*). However, they can often be unequivocally identified through their attachment to specific skeletal elements. In wild-type fetuses, the superficial and lateral masseter is inserted in the lateral aspect of the mandible (Fig. 1*D*), whereas the deep masseter passes through the infraorbital foramen to insert into the medial aspect of the mandible. In *EdnRA*$^{-/-}$, the situation is different; all components of the masseter pass through the infraorbital foramen of the transformed lower jaw (see black arrowhead Fig. 1*B*) and have a large insertion in the medial aspect of this bone. In *EdnRA*$^{-/-}$, the pterygoid and temporal muscles are indistinguishable and form a single muscular mass (Fig. 1*E*). PA2-derived muscles are reduced whereas oculo-motor muscles are normal.

In both *EdnRA*$^{-/-}$ and *Dlx5/6*$^{-/-}$ mice, intrinsic muscles of the tongue and sublingual muscles are severely affected: the genioglossus and the geniohyoid are absent, and other intrinsic muscles of the tongue are reduced and disorganized, thus making the tongue a vestigial medially located structure (Fig. 1 *B*, *B″*, *C*, *C″*, *E′*, and *F′* and Fig. S2 *B*, *E*, and *H*). The mylohyoid and digastric muscles are absent and are replaced by reticular connective tissue with only a few identifiable muscles fibers (Fig. 1 *B‴* and *C‴* and Fig. S2 *C*, *F*, and *I*). To understand the ontogeny of these muscular defects, we then analyzed the myogenic developmental process in *EdnRA*$^{-/-}$ and *Dlx5/6*$^{-/-}$ mutant embryos.

Craniofacial Myogenesis Is Initiated in the Absence of *Dlx5* and *Dlx6* During Early Development. Craniofacial muscle formation initiates with the comigration of CNCCs and the myogenic mesoderm toward PA1 and PA2 (26). The initial stage of specification is characterized by the activation of *Tbx1* and *Capsulin* specifically in head myogenic lineages (15, 27). In contrast, tongue muscles are generated from the rostral migration of myoblasts deriving from the first five somites. The first stages of craniofacial myogenesis are not affected in *Dlx5/6*$^{-/-}$ embryos. Although the shape of *Dlx5/6*$^{-/-}$ PA1 is already slightly altered at E9.5, the migration and initial specification of head myogenic mesoderm is taking place, as shown by the mesodermal activation of *Tbx1* and *Capsulin* at E9.5 in PA1 and PA2 (Fig. 2 *A–D*). Furthermore, migration of somitic tongue muscle precursors along the hypoglossal cord is not altered, as shown by the expression pattern of *Pax3* at E10.5 (Fig. 2 *E–F*).

***Dlx5* and *Dlx6* Expression by CNCCs Is Required for Determination, Differentiation, and Patterning of Craniofacial Muscles.** The initial stages of craniofacial muscle determination are characterized by expression of *Myf5* (28). To follow the onset of myogenic determination, we used *Myf5*$^{nLacZ/+}$ reporter embryos (29). At E10.5, *Myf5-LacZ* is expressed in the extraocular premuscle mass (peom) and in the mandibular arch myoblasts, which later develop into masticatory premuscle masses (pmm) at E11.5–E12.5 (Fig. 3 *A*, *C*, and *E*). In E10.5–E11.5 *Dlx5/6*$^{-/-}$;*Myf5*$^{nLacZ/+}$ embryos, *Myf5-LacZ* expression is strongly reduced in the ocular and masticatory region (Fig. 3 *B* and *D*) and is barely detectable at E12.5 (Fig. 3*F*), indicating a defect in myogenic determination.

The myogenic determination factor *MyoD* is under the control of both the Myf5 and Tbx1 (28). In E11.5 wild-type embryos, *MyoD* is expressed in the extraocular and masticatory premuscle masses; this territory of *MyoD* expression is preserved, but reduced in both *EdnRA*$^{-/-}$ and *Dlx5/6*$^{-/-}$ embryos (Fig. 4 *A–C*).

At later stages, in wild-type fetuses, the masticatory premuscle mass at E12.5 and the masseter muscle at E14.5 and E18.5 are MyoD (Fig. 4 *D* and *G*), Desmin (Figs. S3 *A* and *D* and S4*A*), and fast myosin heavy chain (fMHC) (Fig. S4*A′*) positive, indicating that myogenic differentiation is taking place. In *EdnRA*$^{-/-}$ mutants, the presumptive masseter is present and positive for the above-mentioned myogenic markers, but is clearly reduced at E12.5 and E14.5 (Fig. 4 *E* and *H* and Fig. S3 *B* and *E*) and shows a different morphology and orientation at E18.5 (Fig. S4 *B* and *B′*). In the masseter region of *Dlx5/6*$^{-/-}$ mutants, only a few cells express MyoD, Desmin, and fMHC; the few positive myo-

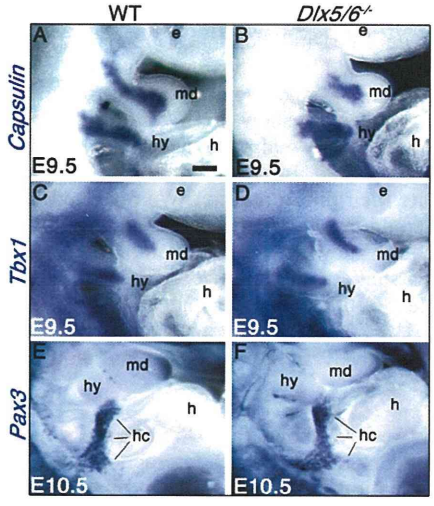

Fig. 2. Expression of early myogenic markers in *Dlx5/6*$^{-/-}$ embryos. Whole-mount in situ hybridization for *Capsulin* (*A* and *B*), *Tbx1* (*C* and *D*), and *Pax3* (*E* and *F*) on E9.5–E10.5 wild-type and *Dlx5/6*$^{-/-}$ embryos. In the mandibular and hyoid arches at E9.5, the expression of the early markers of myogenic specification, *Capsulin* and *Tbx1* (*A–D*), is not affected by the *Dlx5/6* inactivation. The persistence of *Pax3* expression in the hypoglossal cord of E10.5 *Dlx5/6*$^{-/-}$ embryos (*E* and *F*) indicates that somitic myoblast migration during tongue development is not altered. e, eye; h, heart; hc, hypoglossal cord; hy, hyoid arch; md, mandibular arch. (Scale bar: 300 μm in *A–D*; 450 μm in *E* and *F*.)

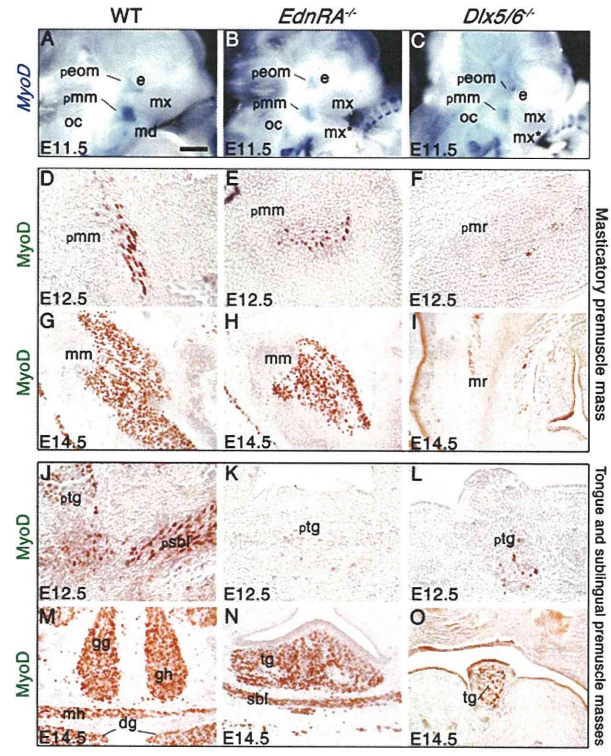

Fig. 4. Expression of *MyoD* in *EdnRA*$^{-/-}$ and *Dlx5/6*$^{-/-}$ mutant embryos. (*A–C*) *MyoD* whole-mount in situ hybridization on E11.5 wild-type (*A*), *EdnRA*$^{-/-}$ (*B*), and *Dlx5/6*$^{-/-}$ (*C*) embryos. *MyoD* expression in the masticatory premuscle mass (pmm) (*A*) is reduced in *EdnRA*$^{-/-}$ and *Dlx5/6*$^{-/-}$ mutants (*B* and *C*). (*D–O*) MyoD immunostaining on frontal sections in the masseter (*D–I*) and tongue (*J–O*) region of wild-type (*D*, *G*, *J*, and *M*), *EdnRA*$^{-/-}$ (*E*, *H*, *K*, and *N*), and *Dlx5/6*$^{-/-}$ embryos (*F*, *I*, *L*, and *O*) at E12.5 (*D–F* and *J–L*) and E14.5 (*G–I* and *M–O*). In *EdnRA*$^{-/-}$ mutants, the masticatory and masseter muscle mass (*E* and *H*) are MyoD positive, but are reduced and show an abnormal morphology. In the *Dlx5/6*$^{-/-}$ mutant, only a few cells express MyoD in the masseter region (*F* and *I*), resulting in an absence of masticatory muscle masses. In *EdnRA*$^{-/-}$ and *Dlx5/6*$^{-/-}$ mutants at E12.5, only a few cells express MyoD in the tongue and sublingual region (*K* and *L*). At E14.5, the myogenic marker is expressed in the vestigial tongue of the two mutants (*N* and *O*), the genioglossus and geniohyoid muscles are never present, and sublingual muscles are barely differentiated in *EdnRA*$^{-/-}$ (*N*) and are absent in *Dlx5/6*$^{-/-}$ mutants (*O*). dg, digastric muscle; e, eye; gg, genioglossus; gh, geniohyoid; md, mandibular bud; mh, mylohyoid; mm, masseter muscle; mr, masseter region; mx, maxillary bud; mx*, duplicated maxillary bud; oc, otic capsule; peom, extraocular premuscle mass; pmm, masticatory premuscle mass; pmr, masticatory premuscle region; psbl, sublingual premuscle mass; ptg, tongue premuscle mass; sbl, sublingual muscle; tg, tongue. (Scale bar: 400 μm in *A–C*; 70 μm in *D–F* and *J–L*; 150 μm in *G–I* and *M–O*.)

blasts do not fuse into myotubes, resulting in the absence of masticatory muscle masses (Fig. 4 *F* and *I* and Figs. S3 *C* and *F* and S4 *C* and *C′*). In *EdnRA*$^{-/-}$ and in *Dlx5/6*$^{-/-}$ mutants, we find expression of muscle determination and differentiation markers in the vestigial tongue from E12.5 to E18.5 (Fig. 4 *J–O* and Figs. S3 *G–L* and S4 *D–F* and *D′–F′*), the genioglossus muscle is never present, and sublingual muscles are barely differentiated (Fig. 4 *K*, *L*, *N*, and *O* and Fig. S3 *H*, *I*, *K*, and *L*).

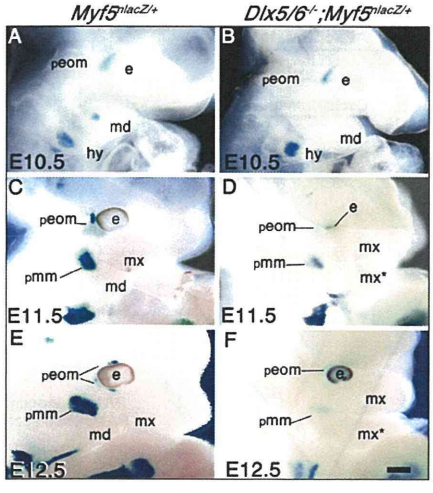

Fig. 3. β-Galactosidase staining on E10.5, E11.5, and E12.5 *Myf5*$^{nLacZ/+}$ and *Dlx5/6*$^{-/-}$;*Myf5*$^{nLacZ/+}$ mutant embryos. In E10.5 *Myf5*$^{nLacZ/+}$ embryos, *Myf5-LacZ* is expressed in the extraocular premuscle mass and in the mandibular and hyoid arches (*A*). At this stage, the expression of *Myf5-LacZ* is not perturbed by *Dlx5/6* inactivation in the hyoid and extraocular region, but is reduced in the mandibular arch (*B*). At E11.5 and E12.5 in *Myf5*$^{nLacZ/+}$ embryos, *Myf5-LacZ* is expressed in the extraocular and masticatory premuscle masses (*C* and *E*). This expression is dramatically reduced in the ocular and mandibular region of *Dlx5/6*$^{-/-}$;*Myf5*$^{nLacZ/+}$ mutant embryos (*D* and *F*). e, eye; hy, hyoid arch; md, mandibular arch; mx, maxillary bud; mx*, duplicated maxillary bud; peom, extraocular premuscle mass; pmm, masticatory premuscle mass. (Scale bar: 500 μm in *A* and *B*; 650 μm in *C* and *D*; 750 μm in *E* and *F*.)

The presence of masticatory muscles in *EdnRA*$^{-/-}$ demonstrates that they can form even in the presence of the lower-to-upper jaw transformation that occurs in both *EdnRA*$^{-/-}$ and *Dlx5/6*$^{-/-}$ mutants. An explanation for the muscle development in *EdnRA*$^{-/-}$ embryos can be found by analyzing the Edn1-independent expression of *Dlx5/6*. Inactivation of *EdnRA* completely prevents the activation of *Dlx5* and *Dlx6* in E9.5 PA1 during CNCC specification. However, in the same mutant at E10.5, *Dlx5/6* are expressed in an Edn1-independent territory in the proximal part of PA1 (25). Similarly, in E11.5 *EdnRA*$^{-/-}$ mutants, distal expression of *Dlx5* and *Dlx6* is lost in the arches, but is maintained in the proximal part of the mandibular and

DEVELOPMENTAL BIOLOGY

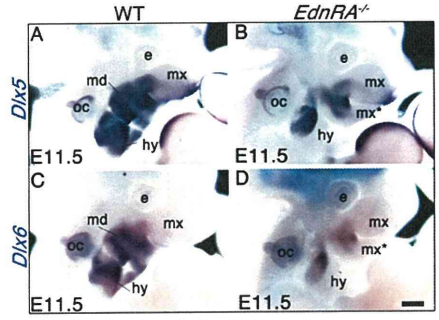

Fig. 5. Whole-mount in situ hybridization on E11.5 wild-type (*A* and *C*) and *EdnRA*$^{-/-}$ (*B* and *D*) embryos using *Dlx5* (*A* and *B*) and *Dlx6* (*C* and *D*) probes. In wild-type embryos (*A* and *C*), *Dlx5* and *Dlx6* are expressed in the mandibular and the hyoid arches and in the proximal part of the maxillary bud. In *EdnRA*$^{-/-}$ mutants, expression of *Dlx5* and *Dlx6* is lost in distal but not in proximal pharyngeal arches, including the duplicated maxillary bud (mx*), the hyoid arch (hy), and the maxillary bud (mx) (*B* and *D*). In these mutants, the pattern of *Dlx5* and *Dlx6* expression in the maxillary bud is a mirror image of that found in the duplicated maxillary bud. e, eye; hy, hyoid arch; md, mandibular arch, mx, maxillary bud; mx*, duplicated maxillary bud; oc, otic capsule. (Scale bar: 650 μm.)

hyoid arches and in the maxillary bud (Fig. 5). Reflecting the mirror transformation of the lower into an upper jaw, at E11.5 the expression of *Dlx5* and *Dlx6* also displays mirror-like symmetry (Fig. 5 *B* and D). Remarkably, in *EdnRA*$^{-/-}$ mutants, the myogenic territory at the origin of masticatory muscles [defined by the expression of *Myf5* (Fig. 3*C*) and *MyoD* (Fig. 4*A*)] is included within the Edn1-independent *Dlx5/6*-positive region, suggesting that the presence of *Dlx5* and *Dlx6* is at the origin of the myogenic differentiation observed in these mutants. Similarly, PA2-derived muscles present milder defects in *EdnRA*$^{-/-}$ than in *Dlx5/6*$^{-/-}$ mutants (Table S1). This might reflect the presence of an Edn1-independent *Dlx5/6*-positive region also within PA2 (Fig. 5). The masticatory muscular defects observed in *EdnRA*$^{-/-}$ and in *Dlx5/6*$^{-/-}$ mutants are summarized in Fig. 6.

In summary, our data show that *Dlx5* and *Dlx6* expression by CNCCs is necessary to maintain the myogenic program in the craniofacial mesoderm. In the absence of *Dlx5/6*, the myoblasts cannot initiate their differentiation. We reasoned that a possible mechanism could involve the derepression of BMP and Wnt signaling, which are known to prevent craniofacial myogenesis (17). Indeed, in a systematic quantitative PCR comparative analysis of microdissected E10.5 wild type and *Dlx5/6*$^{-/-}$ PA1s, we have shown that *BMP7* and *Wnt5a* expression is increased two- and threefold, respectively, in the double-mutant mouse (30).

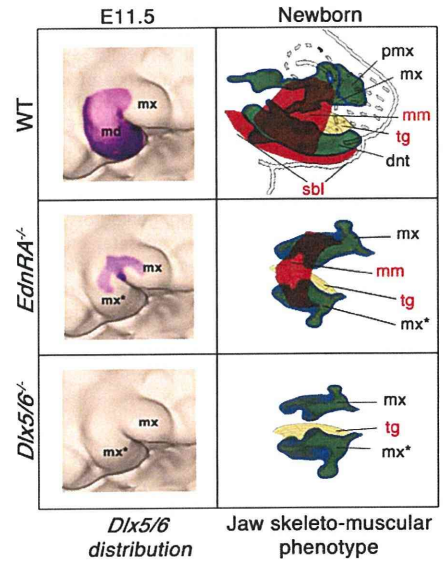

Fig. 6. Summary diagram. (*Left*) The territory of *Dlx5/6* expression in E11.5 PA1 of the three mouse genotypes analyzed in this study. (*Right*) The skeleto-muscular defects observed in these mice are summarized. Muscles are shown as red, bones as green, and the tongue, which is a somite-derived muscle, as yellow. In both *EdnRA*$^{-/-}$ and *Dlx5/6*$^{-/-}$ mutants, lower jaw skeletal elements undergo a mirror image transformation into upper-jaw-like skeletal structures. Although in *EdnRA*$^{-/-}$ mutants the masseter muscle persists, no PA1-derived muscles are differentiated in *Dlx5/6*$^{-/-}$ mutants. dnt, dentary bone; md, mandibular bud; mm, masseter muscle; mx, maxillary bone or maxillary bud; mx*, duplicated maxillary bone or duplicated maxillary bud; pmx, premaxillary bone; sbl, sublingual muscles; tg, tongue.

Discussion

In this study, we have shown that *Dlx5/6* expression by CNCCs is necessary for CNCC–mesoderm interactions resulting in myogenic determination, differentiation, and patterning, but is not required for the early migration and specification of skeletal muscle progenitors. Our findings provide insight on the evolution of the "new head" (1), shedding light on the mechanism at the origin of the muscularized oral apparatus in vertebrates (Fig. 7).

Vertebrate heads share several similar morphological features: multiple brain divisions, pharyngeal arches, migrating CNCCs, sensory placodes, head muscles deriving from unsegmented cephalic mesoderm (31), and a cartilaginous endoskeleton deriving from pharyngeal CNCCs (32).

Although the primordial role of *Dlx* genes in chordates has been the control of appendage development (33), in vertebrates, including gnatostomes and agnathans, these genes are also expressed in the PAs. Particularly, the expression of *Dlx* genes in the PA1 by *Hox*-negative CNCCs (2) is central for the development of oral cartilages (19, 34). Gnathostomes and agnathans differ, however, in the number and pattern of expression of *Dlx* genes in the head. In lampreys, the four *Dlx* genes are uni-

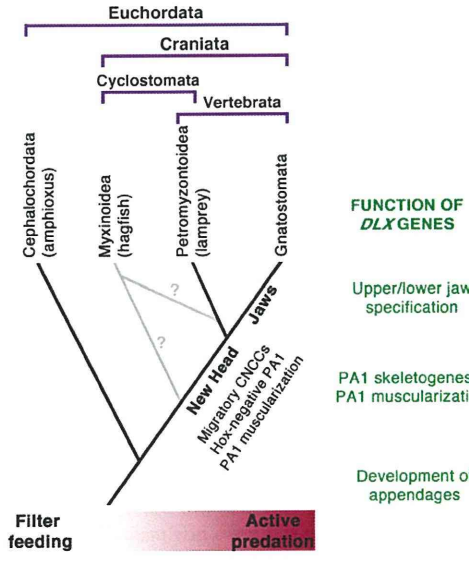

Fig. 7. Roles of *Dlx* genes during chordate evolution. The "new head" characterized by the simultaneous appearance of migratory skeletogenic CNCCs, *Hox*-negative *Dlx*-positive PA1 and PA1 muscularization may or may not include Myxynoidea (39). In this study, we show that CNCC expression of *Dlx* genes not only determines jaw identity in Gnathostomata, but also plays a role in organizing mouth muscularization in vertebrates. The expression of *Dlx* genes in PA1 CNCCs might have had a determining role in the transition between filter feeding and active predation. CNCCs, cranial neural crest cells; PA1, first pharyngeal arch.

formly expressed by PA1 CNCCs. In gnathostomes, the increased number of PA1 *Dlx* genes goes hand-in-hand with the appearance of a dorso-ventral patterning of the branchiomeres at the origin of jaws (20, 32, 34, 35).

Here we show that *Dlx* expression endowed migratory CNCCs with the new function of coordinating cranial skeletogenesis and myogenesis (Fig. 7). It may be wondered whether the role of *Dlx* genes as organizers of a muscularized mouth in vertebrates is distinct from their function in maxillo-mandibular jaw specification in gnathostomes. Although in $Dlx5/6^{-/-}$ mice all masticatory muscles are lost, they are still present in $EdnRA^{-/-}$ mutants. Because these two mutants present a similar lower jaw transformation, we deduce that the capacity of *Dlx* genes to specify jaw identity is distinct from their role in coordinating oral muscularization. Remarkably, in *EdnRA* mutant mice, the masticatory muscles are adapted to the new skeletal morphology reflecting the mirror transformation of the jaws. *Dlx* genes might have had a central role in the harmonious coordination of the oral skeletal and muscular morphogenesis necessary to support the rich craniofacial shape diversity noted in vertebrates. Moreover, it appears that head mesodermal development in lampreys might correspond to the ancestral state of the gene regulatory mechanism at the origin of the vertebrate head (31).

We conclude that the role of *Dlx* genes in defining gnathostome jaw identity might be secondary to a more primitive function in the genesis of the oral skeletomuscular system in vertebrates. Expression of *Dlx* genes in the cephalic region therefore might have had a determining role in the transition between filter feeding and active predation.

Materials and Methods

Mice. *EdnRA* and *Dlx5;Dlx6* mutant mice were genotyped by PCR using allele-specific primers as reported (20, 36). Embryos were fixed in PBS (Sigma) 4% paraformaldehyde (E9.5–E12.5) for 1 d or in Bouin's fixative solution (75% saturated picric acid, 20% formol 40%, 5% acetic acid) for 5 d (E14.5 and E18.5). E18.5 fetuses were decalcified for 2 d with Jenkin's solution (50 mL, 2 d, three changes, 4% hydrochloric acid 37%, 3% acetic acid, 10% chloroform, 10% dH2O, 73% absolute ethanol). Fixed embryos and fetuses were embedded in paraffin and sectioned at 8–12 μm. Serial sections of E18.5 fetuses were subjected to Mallory trichromic staining (22) for anatomical analysis.

$Dlx5/6^{+/-};Myf5^{nLacZ/+}$ heterozygous parents, obtained by crossing $Myf5^{nLacZ/+}$ transgenic males (29) with heterozygous $Dlx5/6^{+/-}$ females, were crossed with $Dlx5/6^{+/-}$ mice to obtain $Myf5^{nLacZ/+}$, $Dlx5/6^{+/-};Myf5^{nLacZ/+}$, and $Dlx5/6^{-/-};Myf5^{nLacZ/+}$ embryos, which were then fixed in PBS 4% PFA and stained to reveal *LacZ* expression.

Immunohistochemistry. Immunohistochemistry was performed on deparaffinized sections using standard protocols of the Dako Envision kit and the Dako ARK kit. Polyclonal rabbit primary antibodies (anti-MyoD; Santa Cruz C-20:sc-304, 1/1200) and anti-Desmin (Abcam AB15200, 1/800) or mouse monoclonal primary antibody (anti-fMHC; Sigma MY-32, 1/100) were diluted in PBS, 1% BSA (Sigma).

Whole-Mount in Situ Hybridization. Whole-mount in situ hybridization was performed with digoxigenin-labeled RNA probes corresponding to the antisense sequence of murine *Tbx1*, *Capsulin*, *Pax3*, *MyoD*, *Dlx5*, and *Dlx6* (all previously reported in refs. 29, 37, and 38), on E9.5–E11.5 embryos adapting the procedure described by Tajbakhsh (29).

ACKNOWLEDGMENTS. We thank Professor Margaret Buckingham (Institut Pasteur, Paris) for the donation of plasmids and $Myf5^{LacZ/+}$ transgenic male mice and Dr. Eldad Tzahor (Weizmann Institute of Science, Rehovot, Israel) for the donation of *Tbx1* plasmids. We thank Anastasia Fontaine, Brice Bellessort, Vanessa Garnier, and Damien Habert for their excellent technical assistance. Particular thanks go to Professor Barbara Demeneix and Dr. Yorick Gitton for their very interesting discussion. This work has been supported in part by grants-in-aid by Association Française contre les Myopathies, the Agence Nationale pour la Recherche, projects Gendactyl and DrOS, and European Community Crescendo LSHM-CT-2005-018652. É.H. is a recipient of a doctoral fellowship from the Gendactyl project supported by the Agence National pour la Recherche; K.B. is a recipient of a doctoral fellowship from the French Government (Ministère de la Recherche et des Enseignements Supérieurs).

1. Glenn Northcutt R (2005) The new head hypothesis revisited. *J Exp Zool B Mol Dev Evol* 304:274–297.
2. Takio Y, et al. (2004) Evolutionary biology: Lamprey Hox genes and the evolution of jaws. *Nature* 429:1 p following 262.
3. Horigome N, et al. (1999) Development of cephalic neural crest cells in embryos of Lampetra japonica, with special reference to the evolution of the jaw. *Dev Biol* 207: 287–308.
4. Helms JA, Cordero D, Tapadia MD (2005) New insights into craniofacial morphogenesis. *Development* 132:851–861.
5. Helms JA, Amasha RR, Leucht P (2007) Bone voyage: An expedition into the molecular and cellular parameters affecting bone graft fate. *Bone* 41:479–485.
6. Noden DM, Trainor PA (2005) Relations and interactions between cranial mesoderm and neural crest populations. *J Anat* 207:575–601.
7. Rinon A, et al. (2007) Cranial neural crest cells regulate head muscle patterning and differentiation during vertebrate embryogenesis. *Development* 134:3065–3075.
8. Grenier J, Teillet MA, Grifone R, Kelly RG, Duprez D (2009) Relationship between neural crest cells and cranial mesoderm during head muscle development. *PLoS One* 4:e4381.
9. Tokita M, Schneider RA (2009) Developmental origins of species-specific muscle pattern. *Dev Biol* 331:311–325.
10. Noden DM (1983) The embryonic origins of avian cephalic and cervical muscles and associated connective tissues. *Am J Anat* 168:257–276.
11. Trainor PA, Tan SS, Tam PP (1994) Cranial paraxial mesoderm: regionalisation of cell fate and impact on craniofacial development in mouse embryos. *Development* 120: 2397–2408.
12. Nathan E, et al. (2008) The contribution of Islet1-expressing splanchnic mesoderm cells to distinct branchiomeric muscles reveals significant heterogeneity in head muscle development. *Development* 135:647–657.
13. Mootoosamy RC, Dietrich S (2002) Distinct regulatory cascades for head and trunk myogenesis. *Development* 129:573–583.
14. Hadchouel J, et al. (2000) Modular long-range regulation of Myf5 reveals unexpected heterogeneity between skeletal muscles in the mouse embryo. *Development* 127: 4455–4467.
15. Lu JR, et al. (2002) Control of facial muscle development by MyoR and capsulin. *Science* 298:2378–2381.
16. Kelly RG, Jerome-Majewska LA, Papaioannou VE (2004) The del22q11.2 candidate gene Tbx1 regulates branchiomeric myogenesis. *Hum Mol Genet* 13:2829–2840.
17. Tzahor E, et al. (2003) Antagonists of Wnt and BMP signaling promote the formation of vertebrate head muscle. *Genes Dev* 17:3087–3099.
18. Couly G, Grapin-Botton A, Coltey P, Ruhin B, Le Douarin NM (1998) Determination of the identity of the derivatives of the cephalic neural crest: Incompatibility between Hox gene expression and lower jaw development. *Development* 125: 3445–3459.
19. Depew MJ, Simpson CA, Morasso M, Rubenstein JL (2005) Reassessing the Dlx code: The genetic regulation of branchial arch skeletal pattern and development. *J Anat* 207:501–561.
20. Beverdam A, et al. (2002) Jaw transformation with gain of symmetry after Dlx5/Dlx6 inactivation: mirror of the past? *Genesis* 34:221–227.
21. Depew MJ, Lufkin T, Rubenstein JL (2002) Specification of jaw subdivisions by Dlx genes. *Science* 298:381–385.
22. Sato T, et al. (2008) An endothelin-1 switch specifies maxillomandibular identity. *Proc Natl Acad Sci USA* 105:18806–18811.
23. Ruest LB, Hammer RE, Yanagisawa M, Clouthier DE (2003) Dlx5/6-enhancer directed expression of Cre recombinase in the pharyngeal arches and brain. *Genesis* 37:188–194.
24. Ruest LB, Xiang X, Lim KC, Levi G, Clouthier DE (2004) Endothelin-A receptor-dependent and -independent signaling pathways in establishing mandibular identity. *Development* 131:4413–4423.
25. Ozeki H, Kurihara Y, Tonami K, Watatani S, Kurihara H (2004) Endothelin-1 regulates the dorsoventral branchial arch patterning in mice. *Mech Dev* 121:387–395.
26. Trainor PA, Tam PP (1995) Cranial paraxial mesoderm and neural crest cells of the mouse embryo: Co-distribution in the craniofacial mesenchyme but distinct segregation in branchial arches. *Development* 121:2569–2582.
27. Dastjerdi A, et al. (2007) Tbx1 regulation of myogenic differentiation in the limb and cranial mesoderm. *Dev Dyn* 236:353–363.
28. Sambasivan R, et al. (2009) Distinct regulatory cascades govern extraocular and pharyngeal arch muscle progenitor cell fates. *Dev Cell* 16:810–821.
29. Tajbakhsh S, Rocancourt D, Cossu G, Buckingham M (1997) Redefining the genetic hierarchies controlling skeletal myogenesis: Pax-3 and Myf-5 act upstream of MyoD. *Cell* 89:127–138.
30. Vieux-Rochas M, et al. (2010) Spatio-temporal dynamics of gene expression of the Edn1-Dlx5/6 pathway during development of the lower jaw. *Genesis*, 10.1002/dvg.20625.
31. Kusakabe R, Kuratani S (2007) Evolutionary perspectives from development of mesodermal components in the lamprey. *Dev Dyn* 236:2410–2420.
32. Kimmel CB, Miller CT, Keynes RJ (2001) Neural crest patterning and the evolution of the jaw. *J Anat* 199:105–120.
33. Panganiban G, et al. (1997) The origin and evolution of animal appendages. *Proc Natl Acad Sci USA* 94:5162–5166.

34. Neidert AH, Virupannavar V, Hooker GW, Langeland JA (2001) Lamprey Dlx genes and early vertebrate evolution. *Proc Natl Acad Sci USA* 98:1665–1670.
35. Graham A (2002) Jaw development: Chinless wonders. *Curr Biol* 12:R810–R812.
36. Kurihara Y, et al. (1994) Elevated blood pressure and craniofacial abnormalities in mice deficient in endothelin-1. *Nature* 368:703–710.
37. Perera M, et al. (2004) Defective neuronogenesis in the absence of Dlx5. *Mol Cell Neurosci* 25:153–161.
38. Tirosh-Finkel L, Elhanany H, Rinon A, Tzahor E (2006) Mesoderm progenitor cells of common origin contribute to the head musculature and the cardiac outflow tract. *Development* 133:1943–1953.
39. Nicholls H (2009) Evolution: Mouth to mouth. *Nature* 461:164–166.

Supporting Information

Heude et al. 10.1073/pnas.1001582107

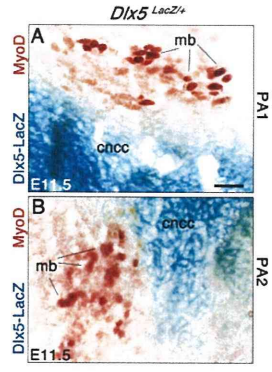

Fig. S1. β-Galactosidase staining and MyoD immunostaining in the PA1 (*A*) and PA2 (*B*) region of the E11.5 *Dlx5*$^{LacZ/+}$ mutant embryo. The stainings show that Dlx5-LacZ is not expressed in the MyoD-positive myoblasts in the PA1 and PA2 region. cncc, cranial neural crest cells; PA1 and PA2, first and second pharyngeal arch; mb, myoblasts. (Scale bar: 20 μm.)

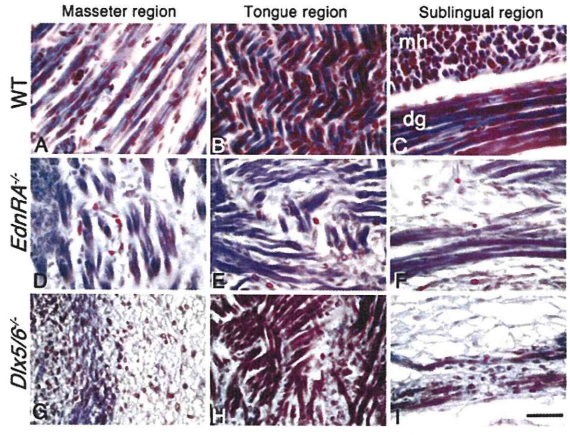

Fig. S2. High magnifications of frontal sections of E18.5 wild-type (*A–C*), *EdnRA*$^{-/-}$ (*D–F*), and *Dlx5/6*$^{-/-}$ (*G–I*) mice stained by Mallory trichromic. High magnifications of the masseter region show a difference of fiber orientation in *EdnRA*$^{-/-}$ fetuses (*D*). We can observe that the masseter is replaced by connective tissue in *Dlx5/6*$^{-/-}$ mice (*G*). In both *EdnRA*$^{-/-}$ (*E*) and *Dlx5/6*$^{-/-}$ (*H*) mutants, the tongue region shows that intrinsic tongue muscle fibers are disorganized. In the sublingual region of the two mutants (*C*, *F*, and *I*), the mylohyoid and the digastric muscles are strongly reduced or absent and replaced by connective tissue where only a few muscle fibers are present. dg, digastric muscle; mh, mylohyoid muscle. (Scale bar: 60 μm.)

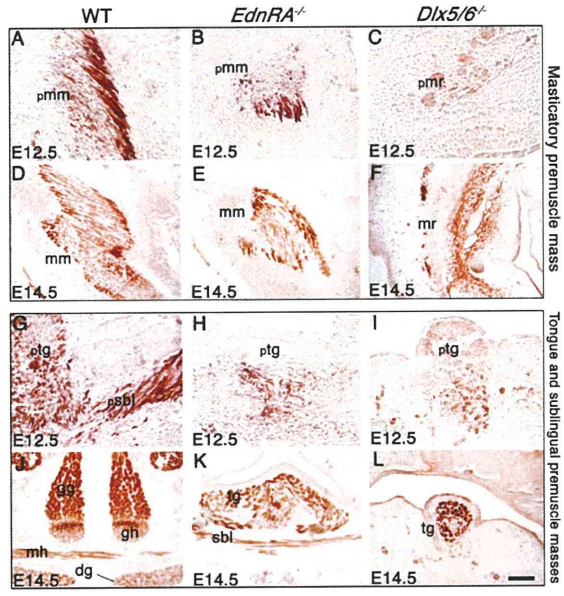

Fig. S3. Desmin immunostaining on frontal sections in the masseter (*A–F*) and tongue region (*G–L*) of wild-type (*A*, *D*, *G*, and *J*), *EdnRA*$^{-/-}$ (*B*, *E*, *H*, and *K*), and *Dlx5/6*$^{-/-}$ (*C*, *F*, *I*, and *L*) mutant embryos at E12.5 (*A–C* and *G–I*) and E14.5 (*D–F* and *J–L*). In *EdnRA*$^{-/-}$ mutants, the masticatory and masseter muscle mass are Desmin-positive (*B* and *E*), but are reduced and show an abnormal morphology. In the *Dlx5/6*$^{-/-}$ mutant, only a few cells express Desmin in the masseter region (*C* and *F*), resulting in an absence of masticatory muscle masses. In *EdnRA*$^{-/-}$ and *Dlx5/6*$^{-/-}$ mutants at E12.5, only a few cells express Desmin in the tongue and sublingual region (*H* and *I*). At E14.5, the myogenic marker is expressed in the vestigial tongue of the two mutants, the genioglossus and geniohyoid muscles are never present, and sublingual muscles are barely differentiated in *EdnRA*$^{-/-}$ (*K*) or are absent in *Dlx5/6*$^{-/-}$ mutants (*L*). dg, digastric muscle; gg, genioglossus; gh, geniohyoid; mh, mylohyoid; mm, masseter muscle; mr, masseter region; pmm, masticatory premuscle mass; pmr, masticatory premuscle region; psbl, sublingual premuscle mass; ptg, tongue premuscle mass; sbl, sublingual muscle; tg, tongue. (Scale bar: 70 μm in *A–C* and *G–I*; 150 μm in *D–F* and *J–L*.)

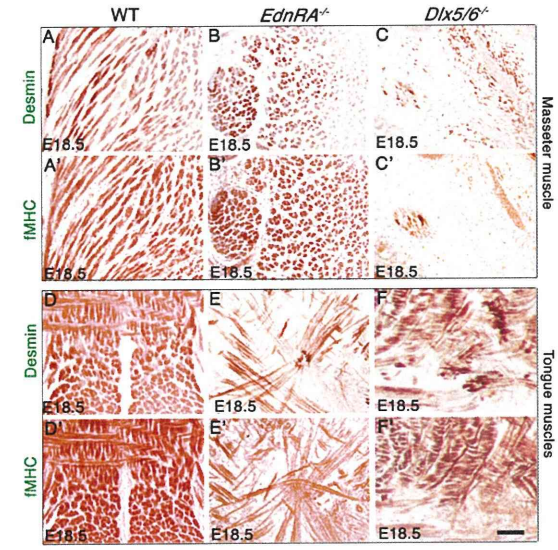

Fig. S4. Desmin (*A–C* and *D–F*) and fMHC (*A′–C′* and *D′–F′*) immunostaining on frontal sections in the masseter (*A–C* and *A′–C′*) and tongue (*D–F* and *D′–F′*) region of E18.5 wild-type (*A*, *A′*, *D*, and *D′*), *EdnRA*$^{-/-}$ (*B*, *B′*, *E*, and *E′*), and *Dlx5/6*$^{-/-}$ (*C*, *C′*, *F*, and *F′*) mutant mice. In E18.5 wild-type fetuses, the masseter muscle (*A* and *A′*) is Desmin and fMHC-positive. In *EdnRA*$^{-/-}$ mutants, the masseter muscle is present and positive for the myogenic markers Desmin and fMHC, but shows a difference of morphology and fiber orientation (*B* and *B′*). In the *Dlx5/6*$^{-/-}$ mutant, only a few cells express Desmin and fMHC in the masseter region (*C* and *C′*), and the myoblasts do not fuse into myofibers, resulting in the absence of masticatory muscle. In wild-type embryos, the tongue is positive for the differentiation markers Desmin and fMHC (*D* and *D′*). In *EdnRA*$^{-/-}$ and *Dlx5/6*$^{-/-}$ mutants, the myogenic markers are expressed in the vestigial tongue of the two mutants (*E*, *E′*, *F*, and *F′*) but intrinsic fibers are dramatically disorganized. (Scale bar: 150 μm.)

Table S1. Head muscle defects in E18.5 *EdnRA*$^{-/-}$ and *Dlx5/6*$^{-/-}$ fetuses

Muscles	Embryonic origin	*EdnRA*$^{-/-}$	*Dlx5/6*$^{-/-}$
Extraocular muscles	Prechordal mesoderm	+++	+
Masticatory muscles			
Temporal	PA1	±	–
Masseter		+	–
Lateral pterygoid		±	–
Median pterygoid		±	–
Facial muscles			
Buccinator	PA2	–	–
Platysma		–	–
Mouth orbicular muscle		±	–
Nasal muscle		±	–
Tongue muscles			
Mylohyoid	PA1	–	–
Anterior digastric		–	–
Posterior digastric	PA2	±	–
Intrinsic muscles of the tongue	Anterior somites (1–5)	±	±

PA1 and PA2, pharyngeal arches 1 and 2; –, absent or few myofibers in the region of the muscle; ±, reduced; +, present but different points of fixation and morphology; +++, normal.

genesis 48:362–373 (2010)

ARTICLE

Spatio-Temporal Dynamics of Gene Expression of the Edn1-Dlx5/6 Pathway During Development of the Lower Jaw

Maxence Vieux-Rochas,[1] Stefano Mantero,[2] Eglantine Heude,[1] Ottavia Barbieri,[3,4] Simonetta Astigiano,[4] Gérard Couly,[1,5] Hiroki Kurihara,[6] Giovanni Levi,[1] and Giorgio R. Merlo[2]*

[1]Evolution des Régulations Endocriniennes, CNRS UMR 7221, Muséum National d'Histoire Naturelle, Paris, France
[2]Dulbecco Telethon Institute, Molecular Biotechnology Center, University of Torino, Torino, Italy
[3]Department of Experimental Medicine, University of Genova, Genova, Italy
[4]Istituto Nazionale per la Ricerca sul Cancro, Genova, Italy
[5]Service de Chirurgie Plastique, Maxillofaciale et Stomatologie, Hôpital Necker-Enfants Malades, Paris, France
[6]Department of Physiological Chemistry and Metabolism, Graduate School of Medicine, University of Tokyo, Tokyo, Japan

Received 26 October 2009; Revised 16 March 2010; Accepted 18 March 2010

Summary: The morphogenesis of the vertebrate skull results from highly dynamic integrated processes involving the exchange of signals between the ectoderm, the endoderm, and cephalic neural crest cells (CNCCs). Before migration CNCCs are not committed to form any specific skull element, molecular signals exchanged in restricted regions of tissue interaction are crucial in providing positional identity to the CNCCs mesenchyme and activate the specific morphogenetic process of different skeletal components of the head. In particular, the endothelin-1 (Edn1)-dependent activation of *Dlx5* and *Dlx6* in CNCCs that colonize the first pharyngeal arch (PA1) is necessary and sufficient to specify maxillo-mandibular identity. Here, to better analyze the spatio-temporal dynamics of this process, we associate quantitative gene expression analysis with detailed examination of skeletal phenotypes resulting from combined allelic reduction of *Edn1*, *Dlx5*, and *Dlx6*. We show that Edn1-dependent and -independent regulatory pathways act at different developmental times in distinct regions of PA1. The Edn1→Dlx5/6→Hand2 pathway is already active at E9.5 during early stages of CNCCs colonization. At later stages (E10.5) the scenario is more complex: we propose a model in which PA1 is subdivided into four adjacent territories in which distinct regulations are taking place. This new developmental model may provide a conceptual framework to interpret the craniofacial malformations present in several mouse mutants and in human first arch syndromes. More in general, our findings emphasize the importance of quantitative gene expression in the fine control of morphogenetic events. genesis 48:362–373, 2010.

Key words: endothelin-1; Dlx; craniofacial development; pharyngeal arches; allelic dosage; cranial neural crest cells; first arch syndromes

INTRODUCTION

Vertebrate jaws are formed through complex morphogenetic processes beginning with the colonization of the first pharyngeal arch (PA1) by *Hox*-negative cephalic neural crest cells (CNCCs) emigrating from the posterior mesencephalic and rhombencephalic neural folds.

Additional Supporting Information may be found in the online version of this article.

Authors' contributions: MV-R carried out mating, pharyngeal arches and skeletal dissections, designed experiments, performed statistical analysis, made figures and prepared the manuscript. SM carried out ISH and quantitative PCR experiments. EH carried out some ISH experiments. OB and SM maintained the animal colony, performed mouse mating and genotyping. GC provided medical expertise and scanners of FAS patients. HK provided Edn1 mutant mice and extensive discussion of the manuscript. GRM carried out ISH, analyzed Real Time PCR data and performed skeletal dissections. GRM and GL designed and coordinated the study, organized the results and prepared the manuscript. All authors read and approved the final manuscript.

Giovanni Levi and Giorgio R. Merlo are co-senior authors.

Abbreviations: CNCCs, cranial neural crest cells; Edn1, endothelin-1; Ednra, endothelin-1 receptor type A; FAS, first arch syndromes; Gsc, goosecoid; PA1, 1st pharyngeal arch; qPCR, quantitative polymerase chain reaction; WT, wild type.

Current address for Maxence Vieux-Rochas: National Research Centre Frontiers in Genetics, School of Life Sciences, Ecole Polytechnique Fédérale (EPFL), Lausanne, Switzerland.

*Correspondence to: Giorgio R. Merlo, Molecular Biotechnology Center, University of Torino, Via Nizza 52, 10126 Torino, Italy.

E-mail: gmerlo@dti.telethon.it

Contract grant sponsors: Telethon Foundation; Cariplo and Compagnia di SanPaolo, Italy; EU Consortium CRESCENDO; French Ministry of Research; Fondation Recherche Médicale; Ministero della Sanità, Italy

Published online 23 March 2010 in
Wiley InterScience (www.interscience.wiley.com).
DOI: 10.1002/dvg.20625

Whereas CNCCs give rise to most chondrocranial and dermatocranial elements of the jaws (Clouthier *et al.*, 1998; Couly *et al.*, 2002; Depew and Simpson, 2006; Kontges and Lumsden, 1996; Ruhin *et al.*, 2003), they do not possess, before migration, the topographic information needed to carry out the jaw morphogenesis (Couly *et al.*, 1993). Surgical removal and grafting of small territories of the foregut endoderm at different developmental stages has shown that this epithelium provides to CNCCs part of the topographic information needed to form jaw structures (Couly *et al.*, 1993; Kontges and Lumsden, 1996; Kurihara *et al.*, 1994; Le Douarin and Dupin, 2003; Noden and Trainor, 2005; Trainor and Tam, 1995). The molecular nature of the endodermal signals is only partly known, as experimental evidence suggest that FGFs, BMPs, Edn1, and Shh are surely involved (Benouaiche *et al.*, 2008; Ozeki *et al.*, 2004; Vieux-Rochas *et al.*, 2007).

In this study, we have analyzed mice with combined and/or partial loss of *Edn1* and *Dlx5;Dlx6* alleles. The Edn1→Dlx5/6→Hand2 signaling is a relevant model to study the spatio-temporal dynamics of gene expression in the PA1 and the consequences for CNCCs specification. Indeed *Edn1* is expressed in the endoderm and in the mesodermal core of the mandibular prominence of PA1, whereas *Ednra (Edn1 receptor-type A)* is broadly expressed by the CNCC-derived PA1 ectomesenchyme and *Dlx5;Dlx6* are only expressed in the mesenchyme of the mandibular prominence (Abe *et al.*, 2007; Clouthier *et al.*, 1998, 2000; Ozeki *et al.*, 2004; Ruest *et al.*, 2004, 2005). Loss of Edn1→Ednra signaling results in the down regulation of the two members of the *distalless* homeobox gene family *Dlx5* and *Dlx6* (Merlo *et al.*, 2002a; Panganiban and Rubenstein, 2002), and in a homeotic-like transformation of lower into upper jaw structures, similar to that observed upon double inactivation of *Dlx5* and *Dlx6* (Beverdam *et al.*, 2002; Depew *et al.*, 2002; Fukuhara *et al.*, 2004; Ruest *et al.*, 2004). The constitutive activation of the Edn1→Ednra signaling in the entire PA1 induces a partial transformation of the upper jaw suggesting that PA1 CNCCs are competent to respond to Edn1 signaling.

Within the PA1 of E10.5 mouse embryos *Dlx* genes are expressed in nested proximo/distal domains: *Dlx1* and *Dlx2* in the proximal and distal maxillary and mandibular prominences, *Dlx5* and *Dlx6* in the entire mandibular prominence, while *Dlx3* only in a medio/distal territory of the mandibular prominence (Depew *et al.*, 2002; Merlo *et al.*, 2000). The most informative data on the role of *Dlx* genes in PA1 patterning come from the analysis of mice carrying single or multiple inactivating mutations for *Dlx1, Dlx2, Dlx5*, and *Dlx6*. In *Dlx5;6* double mutant mice, lower jaw cartilages and bones are transformed and acquire the shape typical of upper jaw elements. Furthermore, in *Dlx5;6* double null mice, *vibrissae* and palatine rugae are symmetrically present in the upper and lower jaw, suggesting that an homeotic transformation has taken place (Beverdam *et al.*, 2002; Depew *et al.*, 2002). In Dlx1;2 double null mice the proximal maxillary region develops abnormal skeletal elements reminiscent of the reptilian upper jaw (Depew *et al.*, 2005; Qiu *et al.*, 1997). These observations have led to the proposition that the combinatorial expression of Dlx genes by PA1 CNCCs determine their relative position and their capacity to give rise to different skeletal elements (Depew and Simpson, 2006; Depew *et al.*, 2005; Merlo *et al.*, 2000).

Several genes have been shown to act downstream of *Dlx5* and *Dlx6*, including *Gsc*, *Pitx1*, *Wnt5a*, *Dlx3*, *Meis2*, and the bHLH transcription factor *Hand2* (Beverdam *et al.*, 2002; Depew *et al.*, 1999, 2002; Merlo *et al.*, 2000, 2002a). A further set of candidate targets of Dlx5/6 have been recently identified (Jeong *et al.*, 2008). Several of the proposed targets might be directly regulated by Dlx5/6 (e.g., *Gbx2, Hand2*) as their promoters harbor Dlx-binding regulatory elements (Charite *et al.*, 2001; Jeong *et al.*, 2008).

Integrating quantitative gene expression data with observed phenotypes we propose that Edn1 signaling occurs in two phases: (1) early in development, Edn1 activates the *Dlx5/6→Hand2* pathway in postmigratory CNCCs. (2) Late in development, distinct regulations can be recognized in distinct regions of the mandibular prominence: in a more proximal region *Dlx5/6* are activated independently from Edn1 and their expression is not associated with *Gsc*. More distally *Dlx5/6* expression depends on Edn1 signaling and results in the activation of downstream genes including *Gsc* and *Pitx1. Hand2* is expressed only in the medio/distal region of the mandibular prominence and its expression depends upon at least three different, regionally restricted, regulations. We conclude that the organization of latero/proximal PA1 structures depends on the quantitative, gene-dosage dependent, regulation of the Edn1→Dlx5/6→(Gsc, Pitx1, etc...) pathway, while medio/distal lower jaw morphology depends on *Hand2* expression. Our findings may also provide the developmental framework in which to elucidate and functionally characterize the molecular lesions, yet to be identified, causing or associated with those human first arch syndromes (FAS) affecting the proximal arch.

RESULTS

Edn1 Allelic Dosage and Dynamics of *Dlx* and *Hand2* Expression in PA1

To better define the role of Edn1/Ednra signaling in the control of mandibular morphogenesis, we examined the effects of allelic reduction of *Edn1* on the expression of key regulators of PA1 patterning. First, we measured by RT-qPCR the abundance of *Dlx2, 3, 5, 6*, and *Hand2* transcripts in the dissected mandibular prominence (the ventral segment of the PA1) of WT and $Edn1^{+/-}$ E9 embryos. At this stage of development CNCCs are still migrating, but most of them have already colonized the mandibular region (Couly *et al.*, 2002; Couly *et al.*, 1993; Le Douarin *et al.*, 2004). In $Edn1^{+/-}$ mandibular

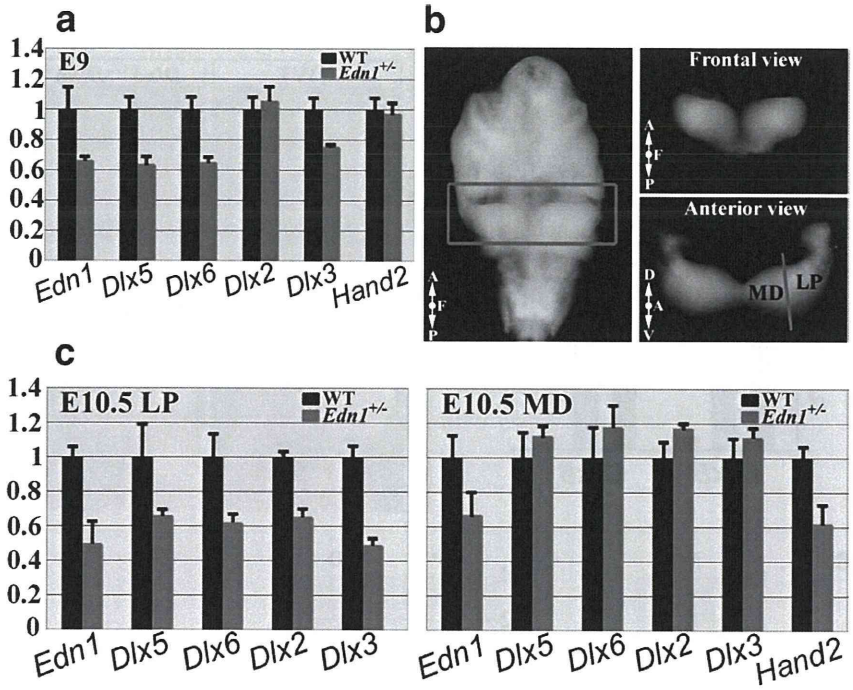

FIG. 1. Effects of allelic reduction of *Edn1* on *Dlx* and *Hand2* gene expression levels in PA1 at E9 and E10.5. (**a**) RT-qPCR measurement of mRNA abundance of *Edn1, Dlx5, Dlx6, Dlx2, Dlx3* and *Hand2* in mandibular prominences from WT (black bars) or $Edn1^{+/-}$ (red bars) at E9. (**b**) Dissection procedure used to separate the LP from the MD part of the mandibular prominence of PA1 at E10.5. The whole mandibular process was first isolated from the embryo and the latero-proximal and medio-distal portions were then separated with a single sharp cut (red line). (**c**) Quantification of the mRNA abundance of *Edn1, Dlx5, Dlx6, Dlx2, Dlx3*, and *Hand2* in LP (left) and MD (right) dissected mandibular prominences from WT (black bars) or $Edn1^{+/-}$ (red bars) at E10.5. WT is set = 1. Axis orientation: A, anterior; D, dorsal; F, frontal; P, posterior; V, ventral. LP, latero-proximal; MD, medio-distal. Black bars represent standard deviation between two independent samples.

prominences, *Edn1* expression was reduced by 38% compared to WT, while *Dlx5, Dlx6*, and *Dlx3* levels were reduced respectively of 35, 36, and 24%. *Dlx2* and *Hand2* were virtually unchanged (Fig. 1a).

Then, we carried out a similar analysis on dissected mandibular prominences obtained from E10.5 WT and $Edn1^{+/-}$ embryos. In this case we further subdivided the mandibular prominence into a latero/proximal (LP) and a medio/distal (MD) segment (as shown in Fig. 1b). In the LP segment, *Dlx2, Dlx3, Dlx5*, and *Dlx6* levels were reduced by 35, 50, 35, and 39%, respectively; *Hand2* expression was very low and was therefore not considered. In the MD segment the levels of expression of *Dlx2*, *Dlx3*, *Dlx5*, and *Dlx6* were not detectably different, while *Hand2* transcripts were reduced by 40% (Fig. 2b). In the LP and MD segments of $Edn1^{+/-}$ mandibular prominences, *Edn1* transcripts were reduced, respectively by 60 and 40% (Fig. 1c).

Thus, loss of one *Edn1* allele reduces the expression levels of *Dlx* genes in E9 mandibular prominences while at E10.5 *Dlx* expression is only reduced in the LP part of the mandibular prominence but not in the MD. However, in the MD portion of the E10.5 mandibular prominence, *Hand2* expression is detectably reduced, suggesting that Edn1 can regulate *Hand2* expression independently from *Dlx* genes.

Expression of *Dlx* Target Genes in the Mandibular Prominence of *Dlx5;Dlx6* Mutant Embryos

In different regions of the mandibular prominence of PA1 Edn1 and Dlx5/6 signaling could act independently. This led us to analyze the quantitative effects of *Dlx5/6* allelic reduction. We first examined how the loss of *Dlx5;Dlx6* alleles affected their own level of mRNA expression. In the mandibular prominence of $Dlx5^{+/-};Dlx6^{+/-}$ embryos *Dlx5* and *Dlx6* mRNAs were reduced, respectively, by 40 and 45%, while in that of $Dlx5^{-/-};Dlx6^{-/-}$ embryos *Dlx5* and *Dlx6* mRNAs were nearly undetectable (Fig. 2a). To further confirm this finding, we performed in situ hybridization. In $Dlx5^{+/-};Dlx6^{+/-}$ embryos we observed a reduced *Dlx5* and *Dlx6* signal in the first and second PA, and in the otic vesicle (Fig. 2b). These results confirm that each allele contributes to the pool of transcripts and that mRNA abundance directly reflects allele dosage.

It has been shown that in the mandibular prominence of $Dlx5^{-/-};Dlx6^{-/-}$ embryos, the expression of many target genes is either up- or down-regulated (Beverdam *et al.*, 2002; Depew *et al.*, 2002; Jeong *et al.*, 2008); in particular it appears that Dlx6 directly activates the transcription of *Hand2* by binding at its promoter (Charite *et al.*, 2001). We determined the expression level of putative *Dlx5;Dlx6* target genes on whole PA1s and on dissected LP and MD segments from embryos with different *Dlx5;Dlx6* allelic

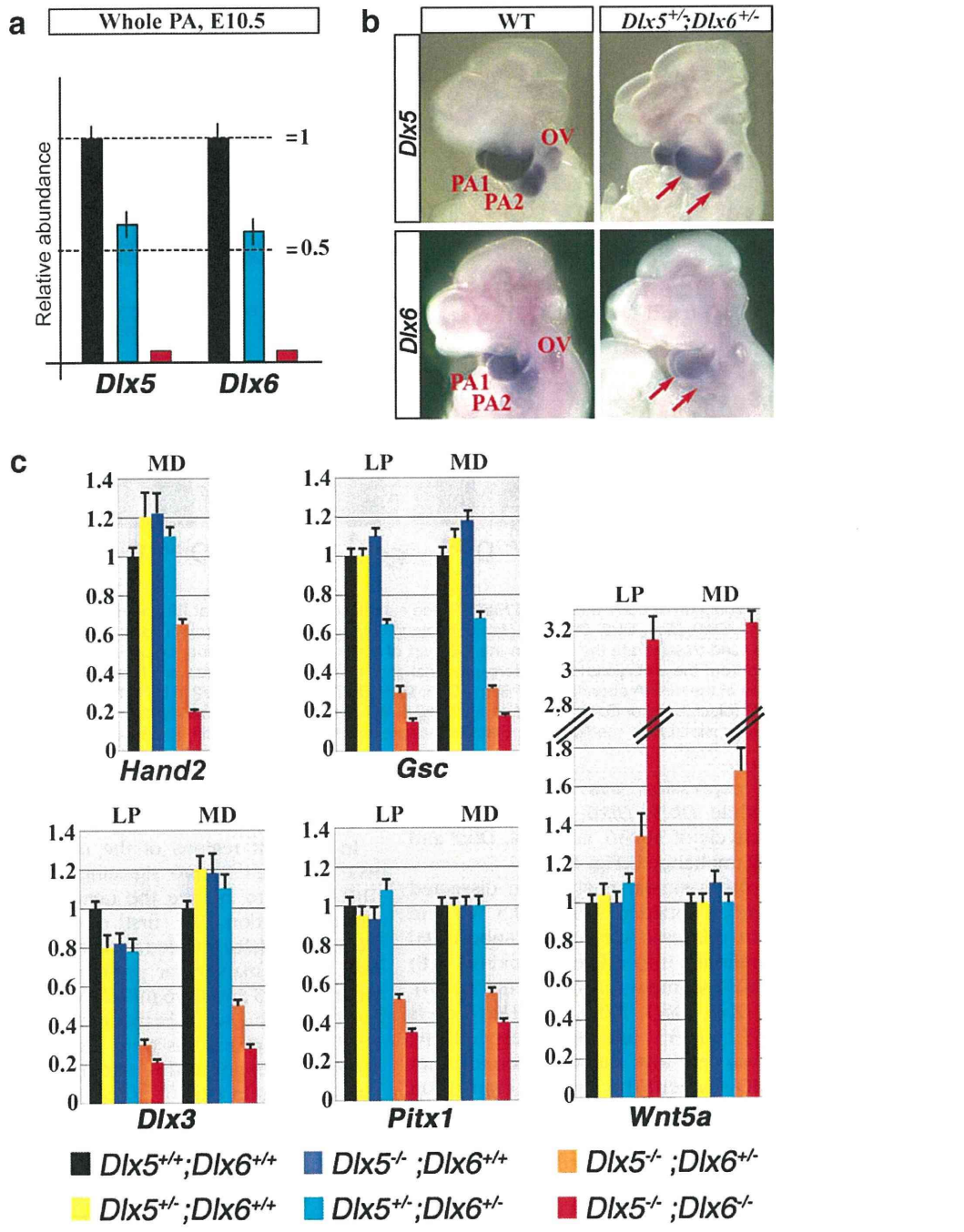

FIG. 2. Effect of allelic reduction of *Dlx5* and *Dlx6* on gene expression levels of target genes in PA1 at E10.5. (**a**) RT-qPCR measurement of *Dlx5* and *Dlx6* transcripts abundance in PA1 of E10.5 WT (black bars), $Dlx5^{+/-};Dlx6^{+/-}$ (blue bars) or $Dlx5^{-/-};Dlx6^{-/-}$ (red bars) embryos. The WT is set = 1, standard deviation is reported. (**b**) In situ hybridization with *Dlx5* (top) and *Dlx6* (bottom) probes on E10.5 WT (left) and $Dlx5^{+/-}$;Dlx6$^{+/-}$ (right) embryos, showing reduction in mRNA levels in the PAs and otic vesicle of heterozygous embryos. (**c**) PA1s were dissected from E10.5 embryos with progressive loss of *Dlx5* and *Dlx6* alleles and further divided into LP and MD regions (see Fig. 1), and stored individually. Samples of similar genotype were pooled. The levels of expression of the *Dlx* targets *Hand2, Pitx1, Dlx3, Gsc*, and *Wnt5a* were measured by RT-qPCR. The results are color-coded by the number of absent *Dlx* alleles. WT is set = 1.

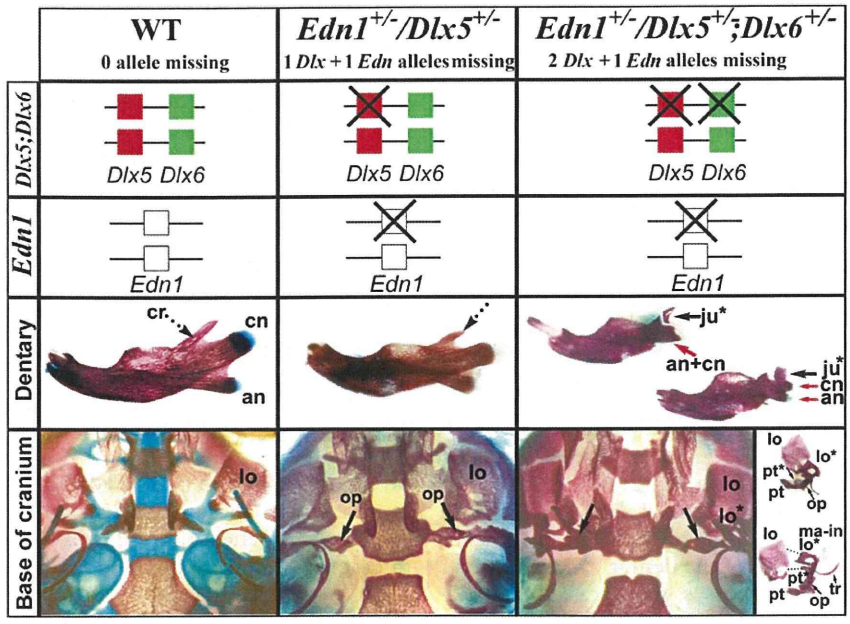

FIG. 3. Allelic reduction of *Dlx5;Dlx6* and *Edn1* results in specific proximal defects. WT, $Edn1^{+/-}/Dlx5^{+/-}$ and $Edn1^{+/-}/Dlx5^{+/-};Dlx6^{+/-}$ newborn mice. Loss of one *Dlx* and one *Edn1* allele results in reduction of the coronoid process of the dentary (dashed arrows) and in the appearance of an extra bone between the pterygoid bone and the middle ear (*os paradoxicum*; green arrows). In $Edn1^{+/-}/Dlx5^{+/-};Dlx6^{+/-}$ mice (right), we observe fusion of the condylar and angular processes (red arrows) of the dentary bone; appearance of duplicated jugal bones in the proximal mandibular arch (black arrows) and the appearance of the *os paradoxicum* (green arrows). Note also the appearance of duplicated structures (asterisks) in the lamina obturans/pterygoid region of the base of the cranium, (further dissociated and shown on the right). *Abbreviations*: an, angular process; cn, condylar process; cr, coronoid process; ds, dentary-squamosal articulation; ju, jugal bone; LO, Lamina Obturans; op, *os paradoxicum*; pt, pterygoid; tb; tympanic bone; tr, tympanic ring; zy, zygomatic arch.

dosage (Fig. 2c, Supporting Information Fig. 1). Both up- (*Wnt5a, Meis2*) and down-regulated (*Hand2*, *Pitx1*, *Dlx3*, and *Gsc*) transcripts were examined.

Similar regulations were observed in the LP and MD subregions, with the exception of *Hand2* whose expression in LP was very low and could not be analyzed by RT-qPCR. Allelic reduction of only one or two *Dlx5/6* alleles did not have detectable effects with the exception of *Gsc*, which was reduced of 35% in both LP and MD regions. Inactivation of three out of four *Dlx5/6* alleles ($Dlx5^{-/-};Dlx6^{+/-}$) resulted in more pronounced regulations: *Hand2* (−35%), *Pitx1* (−45%), *Dlx3* (−50%), *Gsc* (−65%), and *Wnt5a* (+170%). In $Dlx5^{-/-};Dlx6^{-/-}$ embryos: *Hand2* was reduced of 80%, *Pitx1* of 60%, *Dlx3* of 75% *Gsc* of 85% while *Wnt5a* was increased three folds (Fig. 2c). *Meis2* expression was slightly increased (+30%) in the PA1 of $Dlx5^{-/-};Dlx6^{-/-}$ embryos (Supporting Information Fig. 1a) but did not change in all the other genotypes.

The progressive reduction in mRNA abundance of *Hand2* and *Dlx3* in the mandibular prominence of embryos with three or four *Dlx5/6* alleles missing was verified by in situ hybridization. While in $Dlx5^{-/-}$; $Dlx6^{-/-}$ embryos *Hand2* and *Dlx3* expression was below detection, in $Dlx5^{-/-};Dlx6^{+/-}$ embryos we observed a reduced hybridization signal compared to WT embryos (Supporting Information Fig. 1b). These findings suggest that a threshold level of *Dlx5* and *Dlx6* mRNA is necessary to activate target gene transcription.

Craniofacial Phenotypes of Mice With Combined Loss of *Edn1* and *Dlx5;Dlx6* Alleles

Dlx and *Hand2* genes play important roles in the control of craniofacial morphogenesis. As the loss of one *Edn1* allele reduces the expression levels of *Dlx* and *Hand2* genes, we analyzed the skulls of $Edn1^{+/-}$ newborn mice, but no obvious malformation could be detected (not shown); this finding is not surprising as $Dlx2^{+/-}$, $Dlx5^{+/-}$, $Dlx5^{+/-}$; $Dlx6^{+/-}$ and $Hand2^{+/-}$ mice also show only minor craniofacial defects (Acampora *et al.*, 1999; Beverdam *et al.*, 2002; Depew *et al.*, 1999; Robledo *et al.*, 2002; Yanagisawa *et al.*, 2003). As the loss of one *Edn1* allele could further reduce the level of *Dlx5/6* and/or *Hand2* expression, we examined the craniofacial skeleton of combined *Edn1/Dlx* mutant mice. We therefore crossbred $Edn1^{+/-}$ mice with either $Dlx5^{+/-}$ or $Dlx5^{+/-};Dlx6^{+/-}$ mice.

When both one *Edn1* and one *Dlx5* allele were lost, we observed a slightly shorter coronoid process of the dentary and the appearance of an *os paradoxicum* at the base of the cranium, highly reminiscent of that observed in $Dlx5^{+/-};Dlx6^{+/-}$ or in $Dlx5^{-/-}$ or $Dlx6^{-/-}$ mutants; in each of these allelic configurations two *Dlx5/6* alleles are missing (Fig. 3, Supporting Informa-

tion Fig. 4 and Table 1; Jeong *et al.*, 2008). No other obvious defect was observed.

In *Edn1*$^{+/-}$/*Dlx5*$^{+/-}$;*Dlx6*$^{+/-}$ mice we observed a more severe phenotype. The distance between the condylar and angular processes of the dentary was reduced and often these two processes fused into a single large structure, similar to the zygomatic process of the maxilla. The coronoid process was missing and an additional skeletal element was often observed between the abnormal condylar process (lower jaw) and the jugal bone (upper jaw). This new structure could be interpreted as a duplicated jugal bone. At the base of the cranium, the pterygoid and the *ala temporalis* were duplicated and fused with the *os paradoxicum* and positioned ventrally to overlap with the normal structure (see Fig. 3). Collectively, these phenotypes closely resemble those observed in *Dlx5*$^{-/-}$;*Dlx6*$^{+/-}$ animals (three *Dlx* alleles missing; Supporting Information Fig. 2; Beverdam *et al.*, 2002; Depew *et al.*, 2005). Indeed *Dlx5*$^{-/-}$;*Dlx6*$^{+/-}$ mice also display reduced distance or fusion of the condylar and angular processes of the dentary and the lateral extension of the fused processes giving rise to a structure similar to the zygomatic process of the maxilla. In these mice an extra element is also present, which can be interpreted as a duplicated jugal bone and duplication of the pterygoid-ala temporalis-lamina obturans on the mandibular side. Thus, the anomalies seen in *Dlx5*$^{-/-}$;*Dlx6*$^{+/-}$, and in *Edn1*$^{+/-}$/*Dlx5*$^{+/-}$;*Dlx6*$^{+/-}$ newborns affect derivatives of the proximal region of the mandibular segment, while derivatives of the distal region such as the body of the dentary show no major defects. In most embryos these defects were asymmetric, namely the left side of the mandible was more severely affected than the right one (data not shown). In summary: (1) the gradual changes observed in the levels of expression of Dlx5/6 targets correlate well with the progressive onset of specific skeletal anomalies affecting the proximal lower jaw and 2) the reduction of *Edn1* level of transcription, in combination with the loss of one or two *Dlx5;Dlx6* alleles, has phenotypic consequences similar to the loss of one additional *Dlx* allele (Figs. 2 and 3, and Supporting Information Fig. 3).

Remarkably, the defects caused by allelic reduction of *Edn1* and *Dlx5;Dlx6* resemble those present in patients affected by first arch syndromes (FAS) in which only proximal derivatives of PA1 are affected and which often show the presence of ectopic bones positionally homologous to a duplicated jugal (see Discussion).

Effect of *Ednra* and *Dlx5/6* Inactivation on Downstream Targets Expression Pattern

In the mandibular prominence of normal E10.5 embryos, *Dlx5* and *Dlx6* are expressed in a large and coherent territory extending distally from a proximal limit corresponding to the maxillo/mandibular boundary. The distal-most region of PA1, including the medial fusion, does not, however, express *Dlx5* and *Dlx6* (Fig. 4a,c,e,g). Inactivation of *Ednra* completely prevents the expression of *Dlx5* and *Dlx6* in the E9.5 PA1 (Ozeki *et al.*, 2004); in these same mutants at E10.5, however, *Dlx5* and *Dlx6* are expressed in an Edn1-independent territory in the proximal part of PA1 (Fig. 4b,d,f,h black arrows; Ozeki *et al.*, 2004). In normal E10.5 embryos, *Gsc* expression is limited to a distal region of PA1 overlapping in part with the Edn1-dependent territory of *Dlx* activation. *Gsc* expression is abolished in both *Ednra* and *Dlx5/6* mutant mice (Fig. 4i–n). Careful analysis of our embryos revealed an additional territory of *Gsc* expression in the proximal endoderm of PA1 (red arrows, Fig. 5i–k,n), this small territory of expression is independent from both Ednra and Dlx5/6.

DISCUSSION

An emerging theme in developmental biology is the importance of quantitative functions shared by related and coexpressed genes. Examples of these are the signaling functions of FGFs expressed in the apical ectodermal ridge (Mariani *et al.*, 2008), the gene-dosage dependent functions of *Msx1* and *Msx2* for osteogenic differentiation of CNCCs (Han *et al.*, 2007), and the progressive limb phenotypes associated with the combined loss of posterior *HoxD* alleles and with a gradual increase of expression of the HoxD target Epha3 (Cobb and Duboule, 2005). Our study offers a new example in this direction. One implication of this is that the function of individual genes is best examined upon partial and cumulative gene losses, and within the context of expression of related genes. Indeed, the examination of developmental phenotypes in mice homozygous for recessive mutant mice, although widely used, has serious limitations. One of these is the inability to recognize late-occurring regulations (or phenotypes), in case an early event severely affects morphogenesis, patterning or embryonic viability. Second, we cannot appreciate the phenotypic consequences of reduced gene expression; third we may fail to recognize the dynamics of cell–cell signaling and interactions, as these often require a nearly normal context. Such is the case of Edn1→Dlx signaling at the basis of the homeotic lower jaw transformation, to investigate which many studies have been carried out based on either loss-of-function (Acampora *et al.*, 1999; Beverdam *et al.*, 2002; Clouthier *et al.*, 1998; Depew *et al.*, 1999, 2002; Kurihara *et al.*, 1994; Ozeki *et al.*, 2004; Sato *et al.*, 2008a; Thomas *et al.*, 1998; Yanagisawa *et al.*, 2003) or gain-of-function mutants (Sato *et al.*, 2008b). Here we provide quantitative data on the effects of allelic reduction of *Edn1* and *Dlx5;Dlx6* at different developmental stages. Our findings are complementary to those recently reported by Ruest and Clouthier (2009) using CNCC-specific gene deletion and receptor antagonism, and corroborate and extend their major conclusions. We show that, during PA1 development, different Edn1-dependent regulatory pathways act at diverse developmental times in distinct regions of the mandibular prominence. We also show that upon partial

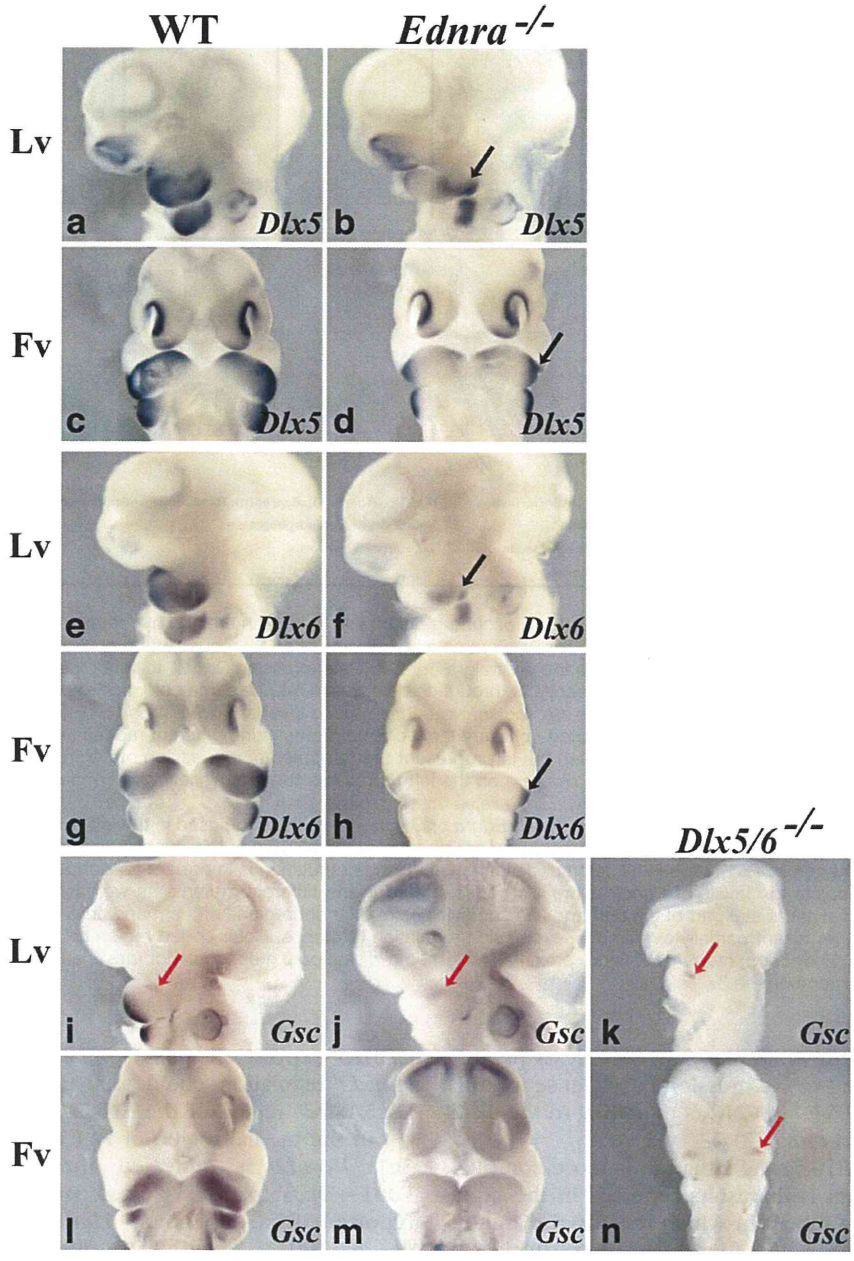

FIG. 4. *Dlx5, Dlx6* and *Gsc* expression in *Ednra* and *Dlx5/6* mutant mice. Whole-mount in situ hybridization on wild-type (**a**,**c**,**e**,**g**,**i**,**l**), *Ednra*$^{-/-}$ (**b**,**d**,**f**,**h**,**j**,**m**) or *Dlx5/6*$^{-/-}$ (**k**,**n**) E10.5 embryos using *Dlx5* (a–d), *Dlx6* (e–h) and *Gsc* (i–n) probes. *Dlx5* and *Dlx6* are expressed in the mandibular part of the PA1 and in the PA2 of wild-type embryos (a,b,e,f). In Ednra homozygous mutants, distal expression of *Dlx5* and *Dlx6* is lost in PA, but is still maintained in the proximal part of PA1 (black arrow) and PA2 (c,d,g,h). In normal embryos, *Gsc* is expressed in a latero-distal region within PA1 and PA2 and in a small endodermal territory located at the mandibulo-maxillary junction (red arrow) (i,l). In *Ednra* and *Dlx5/6* mutant embryos, *Gsc* expression is lost in the distal PA1 and PA2 whereas is still maintained in the endoderm at the mandibulo-maxillary junction (j–n). Fv, Frontal view; Lv, Lateral view.

allele loss, the proximal territory of mandibular prominence is the region mainly affected.

At early stages of CNCCs colonization, Edn1 signaling activates *Dlx5/6* expression in CNCCs; accordingly *Dlx5/6* mRNAs are reduced at E9 in the mandibular prominence of *Edn1* heterozygotes (see Fig. 1). If early Edn1 signaling is abrogated (i.e., in *Edn1* or *Ednra*-null mice), *Dlx5/6* fail to be activated in the entire PA1 at least up to E9.5 (Abe *et al.*, 2007; Ozeki *et al.*, 2004; see Fig. 5). This implies that signals that pattern *Dlx* expres-

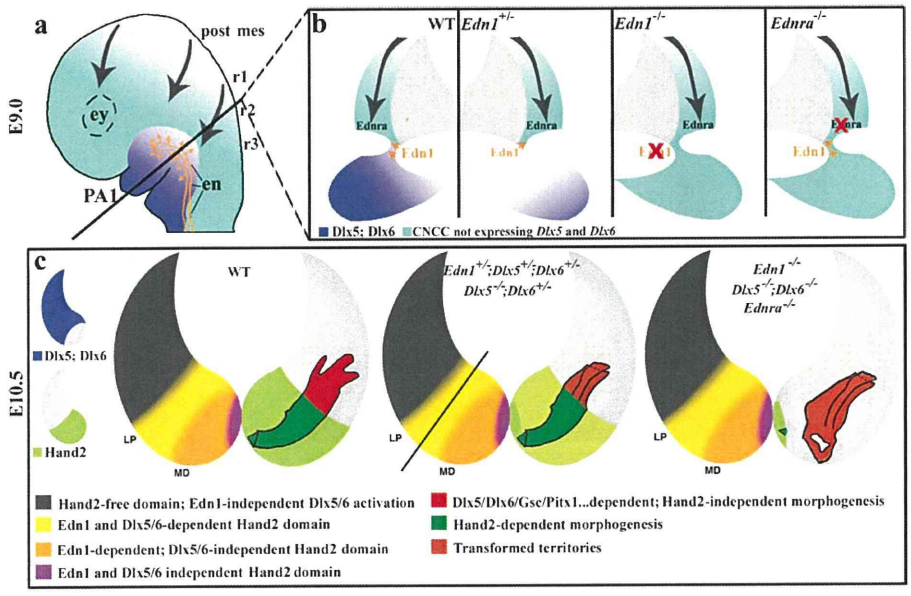

FIG. 5. Summary diagram of Edn1-dependent regulations occurring during PA1 development and hypothetical model for the origin of first arch syndromes. (**a**) Schematic view illustrating CNCCs migration on a lateral view of an E9 mouse embryo. In orange is indicated the endoderm from which *Edn1* signaling originates, in purple the postmigratory CNCCs expressing *Dlx5/6*, in light blue the territory of migration of CNCCs (arrows). (**b**) Drawings represent transverse sections through the embryo in (A), the same color code is used. Sections corresponding to WT, *Edn1*$^{+/-}$, *Edn1*$^{-/-}$ and *Ednra*$^{-/-}$ embryos are shown. Note the reduced level of *Dlx5/6* in *Edn1*$^{+/-}$ embryos and the absence of early *Dlx5/6* activation when Edn1 signaling is disrupted. (**c**) Summary scheme representing different modes and territories of gene activation in E10.5 mandibular prominence. Small inserts on the left represent the territories of expression of *Dlx5/6* (upper, purple) and *Hand2* (lower, light green) respectively in WT embryos. The diagram on the left represents the frontal view of the mandibular part of PA1 of a WT E10.5 embryo. The central diagram refers to three *Dlx/Edn1* alleles missing, either *Dlx5*$^{-/-}$;*Dlx6*$^{+/-}$ or *Edn1*$^{+/-}$/*Dlx5*$^{+/-}$;*Dlx6*$^{+/-}$. Finally the right diagram refers to homozygous mutants for either *Edn1*, *Ednra* or *Dlx5/6*. The color code used in the left side of each drawing indicates the four different regulations observed in PA1 at this stage and are detailed in the caption of this panel. The large grey area corresponds to the Hand2-independent part of PA1, while in all colored, distal regions Hand2 regulation is important for correct morphogenesis. The right part of the diagram depicts the levels of *Hand2* expression encountered in the different mutants as well as the morphogenetic defects occurring in the proximal and distal part of the dentary. The subdivisions of different regions of the mandibular prominence are not divided by actual borders, but represent partially overlapping expression/regulation territories. Color-coded region have faded borders to indicate this. *Abbreviations*: en, endoderm; ey, eye; LP, latero proximal; MD, medio-distal; post mes, posterior mesenchephalon; r1, rhombomere 1; r2, rhombomere 2; r3, rhombomere 3.

sion, such as Edn1 or FGF8 likely act on CNCCs prior to E10.5; for example *Dlx5* expression in response to Edn1 initiates around E8.5-E9 in CNCCs migrating to the distal PA1 (Vieux-Rochas *et al.*, 2007).

At later stages (E10.5) the situation is more complex. Combining our data with results reported in the literature, we propose a model in which the E10.5 mandibular arch is subdivided into four adjacent territories, in which distinct timing and patterns of gene expression are linked to the onset of specific phenotypes (Fig. 5c): (1) in the distal-most region (purple in Fig. 5c), *Hand2* expression is independent from both Edn1 and Dlx5/6. Indeed, *Hand2* expression is retained in a small distal territory in *Edn1*-null, *Ednra*-null and *Dlx5;6*-null animals (Beverdam *et al.*, 2002; Clouthier *et al.*, 2000; Fukuhara *et al.*, 2004; Ozeki *et al.*, 2004; Ruest *et al.*, 2004), possibly associated with the specific fate of this region to undergo midline fusion (Barbosa *et al.*, 2007). (2) in the MD region of PA1, *Hand2* expression can be activated by Edn1 independently of Dlx5/6 as seen from the fact that *Edn1* allelic reduction affects *Hand2*, but not *Dlx5/6* expression (see Fig. 1). This Dlx-independent *Hand2* regulation could well take place in the distal Dlx5/6-free region of the E10.5 PA1 (orange in Fig. 5c). (3) In the medial region of PA1 at E10.5 (yellow in Fig. 5c), *Hand2* is activated through the established Edn1→Dlx6 pathway most probably involving the reported Dlx6-dependent *Hand2* enhancer (Charite *et al.*, 2001). Notably, inactivation of this enhancer results in defects in the medio-distal part of PA1 as suggested by our model (Yanagisawa *et al.*, 2003) and by timed inhibition of Edn1 signaling using Ednra antagonists (Ruest and Clouthier, 2009). (4) Finally, in the proximal part of the E10.5 PA1 (grey in Fig. 5c), *Hand2* is never expressed. Within subterritories of this same region *Dlx5* and *Dlx6* can be activated even in the absence of an Edn1 inducing signal. These different sub-territories could confer a regional selectivity, in turn required for the correct unfolding of the lower jaw morphogenetic program.

Allelic reduction of *Edn1* results in lower *Dlx5/Dlx6* (and *Dlx2* and *Dlx3*) expression in the proximal, but not